Niobium transducers for the Mario Schenberg detector and a Multi-Nested Pendula for use in interferometric detectors

Elvis Camilo Ferreira
Postdoc at CP3, UCLouvain
Louvain-la-Neuve, Belgium
May 11th, 2021

Summary

- Introduction to Gravitational Waves detection
- The Mario Schenberg detector (Scheberg)
- Niobium transducers for Scheberg
- Multi-Nested Pendula for interferometric detectors

Gravitational waves (GW)

- GW are 'ripples' in space-time that travels at at the speed of light.
- They are predicted by Einstein's 1915 general theory of relativity;

$$\Box \bar{h}_{\mu\nu} = -\frac{16\pi G}{c^4} T_{\mu\nu} \quad \Rightarrow \quad \Box \bar{h}_{\mu\nu} = 0 \quad \Rightarrow \quad h_{ij}^{\mathrm{TT}}(t,z) = \begin{pmatrix} h_+ & h_\times & 0 \\ h_\times & -h_+ & 0 \\ 0 & 0 & 0 \end{pmatrix}_{ij} \cos[\omega(t - z/c)]$$

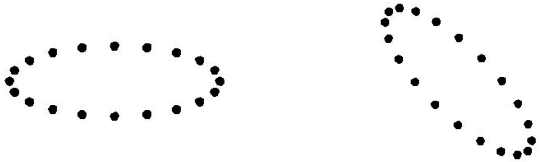

$$h = \sqrt{h_+^2 + h_\times^2} \equiv \Delta L / L$$

Measuring a GW

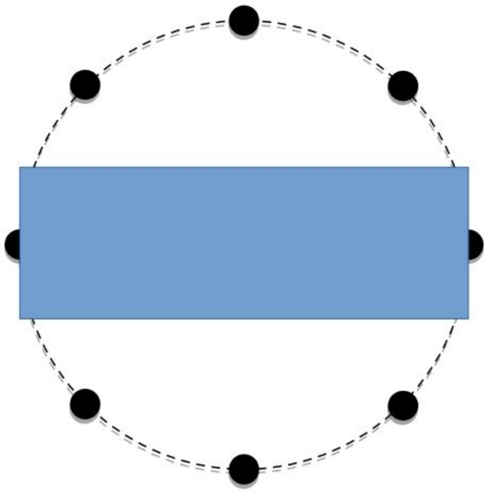

Resonant mass - cylinder

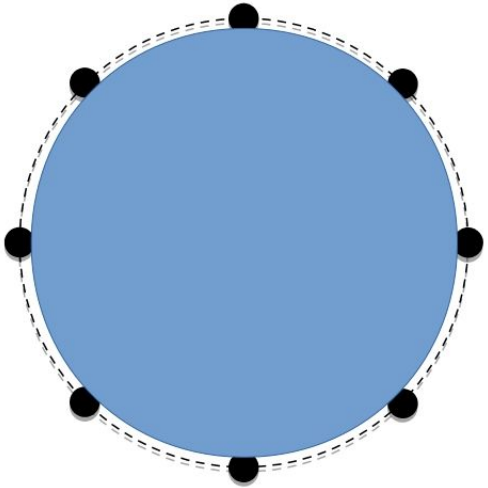

Resonant mass - sphere

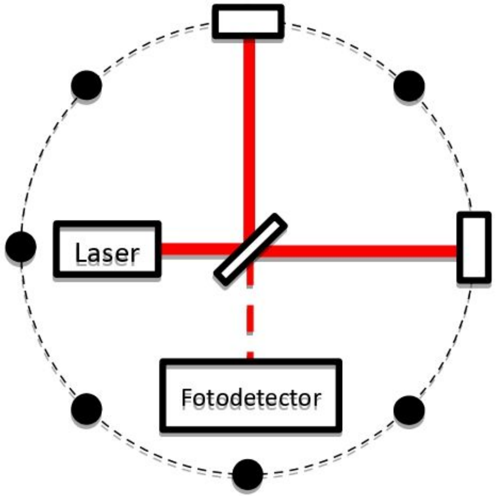

From Shapiro (G1601357-v2)

Interferometer

Mario Schenberg

- It is a cryogenic resonant mass spherical GW detector.
- Cu-Al(6%), 1150 kg, 65 cm diameter.
- It can detect the direction of incident GW.
- Qmec ~ 2×10^6 at T = 2 K.

Mario Schenberg

- Design sensitivity:

$h \approx 1\times10^{-22}\ \mathrm{Hz}^{-1/2}$ at $3200\pm200\ \mathrm{Hz}$

- It has vacuum chambers and cryogenic layers of LN and LHe.
- It could detect dynamic instabilities neutron stars and excitation of vibrational modes of black holes with ~3Ms.

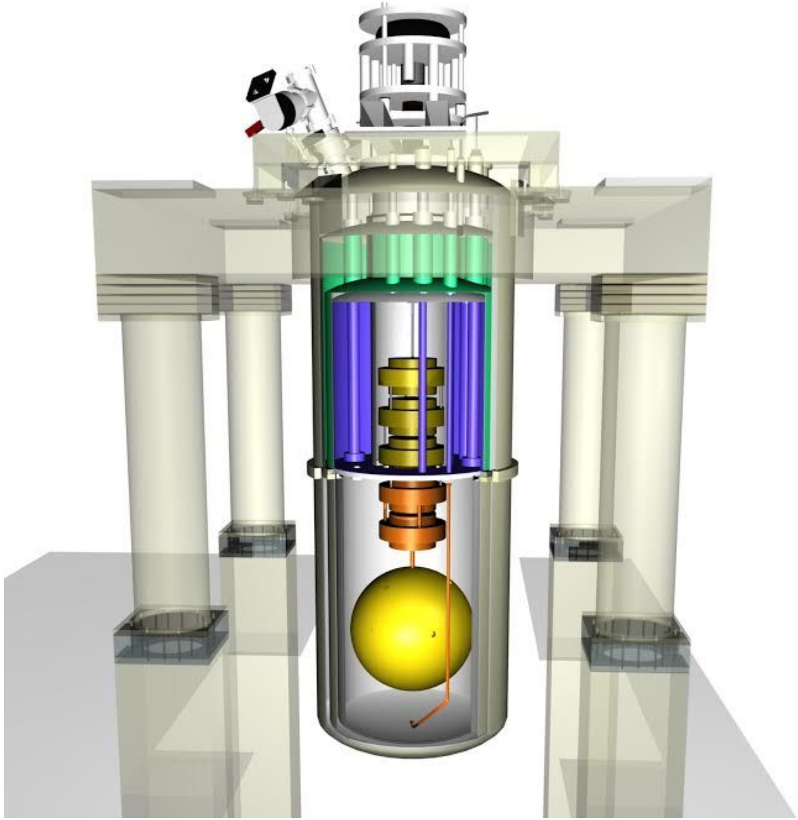

Niobium transducers for Scheberg

To monitor the five quadrupolar modes a set of parametric transducers are coupled with the sphere.

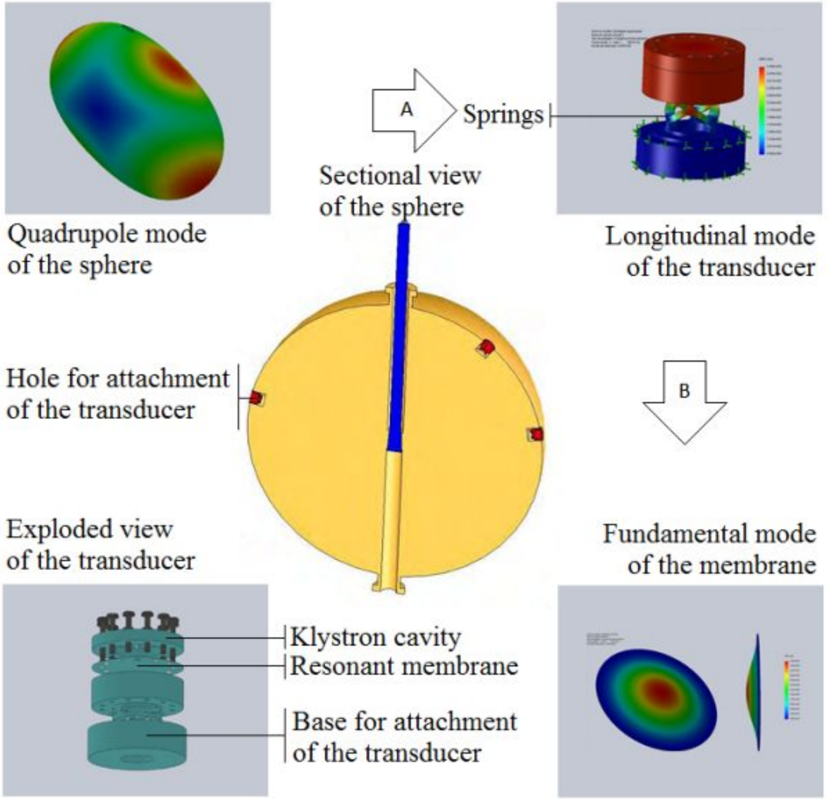

doi:10.1088/1748-0221/10/03/P03001

Niobium transducers for Scheberg

To monitor the five quadrupolar modes a set of parametric transducers are coupled with the sphere.

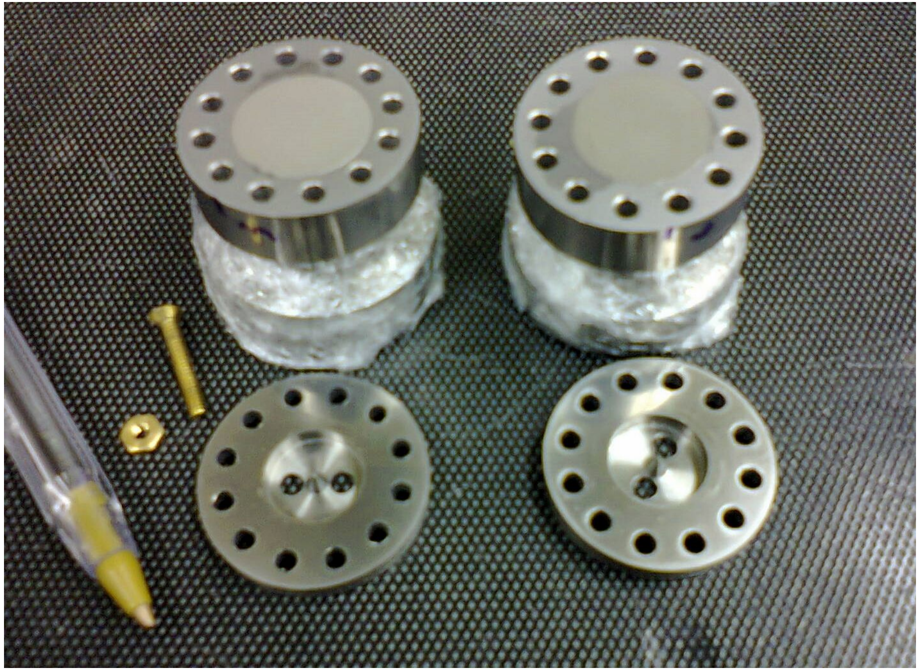

Niobium transducers for Scheberg

They have an mechanical amplitude gain of ~10^4;

The resonance frequency of the membrane is 3.2 kHz.

The microwave cavities: 9.44 GHz, and to have a gap about 3 microns.

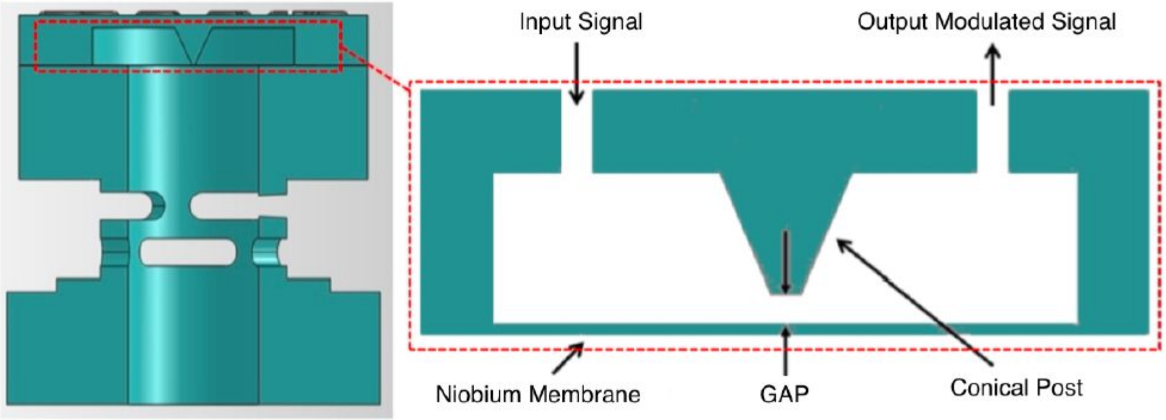

Nb has high mechanical Q-factor and superconductive behaviour at temperatures below 9.2 K, which reduces the electrical losses in the transduction process.

Fine mechanical adjustments to tune the electrical resonance frequencies of the cavities by a process of sanding the cavities of the transducers.

Sample	Cavity Frequencies [GHz]							
	step 1	step 2	step 3	step 4	step 5	step 6	step 7	step 8
1	12.76	12.88	**9.52**	**9.52**	**9.52**	**9.52**	**9.52**	**9.52**
2	12.44	12.32	**9.52**	**9.52**	**9.52**	**9.52**	**9.52**	**9.52**
3	13.40	13.88	13.36	13.16	12.76	12.32	12.06	11.08
4	10.96	10.92	**9.88**	**9.88**	**9.88**	**9.88**	**9.88**	**9.88**
5	13.12	13.28	13.00	12.76	12.64	11.92	11.56	10.54
6	12.64	13.20	12.36	12.00	11.74	12.52	12.20	12.13
7	**9.76**	**9.76**	**9.76**	**9.76**	**9.76**	**9.76**	**9.76**	**9.76**
8	11.28	11.28	10.60	10.08	**9.48**	**9.48**	**9.48**	**9.48**

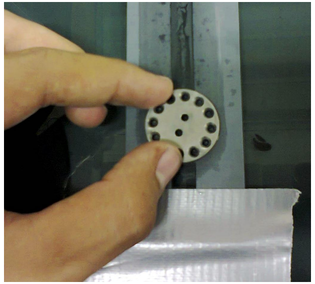

After a process of cleaning, the transducers were measured in a cleanroom.

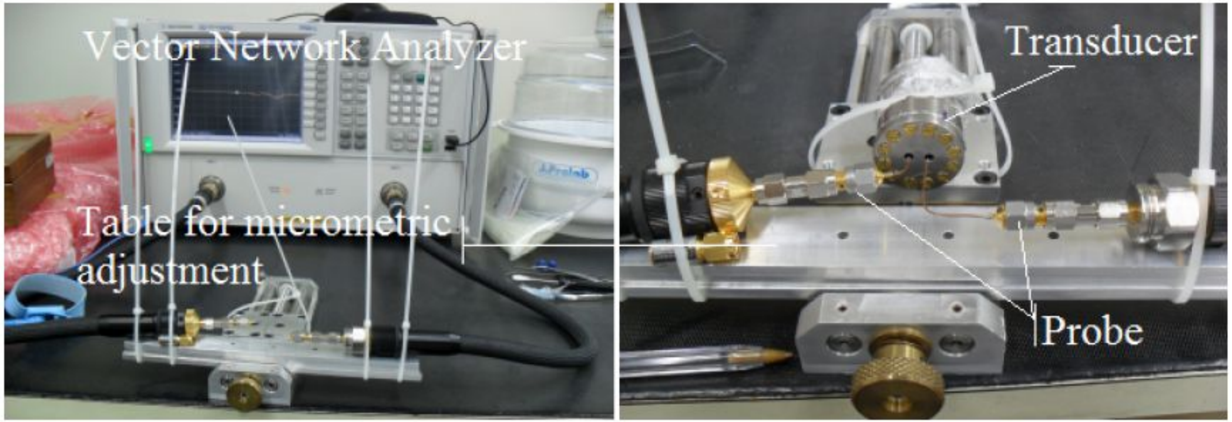

L.A.N. De Paula, et al. High sensitivity niobium parametric transducer for the Mario Schenberg gravitational wave detector. ***JINST 10 P03001***

Schenberg scientific run

In 2015, the maximum sensitivity achieved at the scientific run were ~**10^{-20}/Hz$^{1/2}$** in **3150-3260 Hz** band for one of those transducers, and **~10^{-19}/Hz$^{1/2}$** for the others (Dr. Odylio Aguiar).

Optimization of Qe

- The electric **Q factor determines the performance** of the resonant circuit.
- It is proportional to the **ratio** between the **energy stored and lost** in the circuit per cycle.

- The final goal: **Qe's of 5.0 x 10^5**. This will allow us to reach the quantum limit of detector sensitivity.

- A **Qe of ~100,000** was measured from a cavity treated with a **plasma immersion ion implantation (PIII) of Nitrogen.** V. Liccardo *et al* 2016 *JINST* 11 P07004

- So, we decided to investigate that on some cavities.


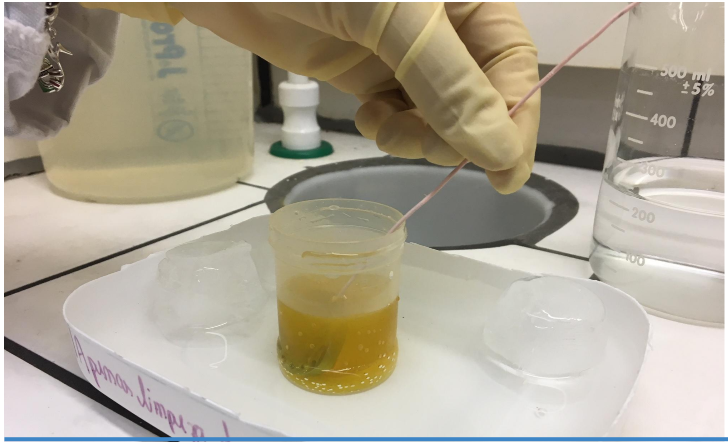

Niobium transducers

- The cavities were submitted to **chemical etching**, being dipped in a solution which composition in volume is as follow: HF (26%), HNO3 (40%) and H3PO4 (34%).
- The aim is to **remove the first layers of the surface** that may have been contaminated during the fabrication process and layers of natural oxide.

Niobium transducers

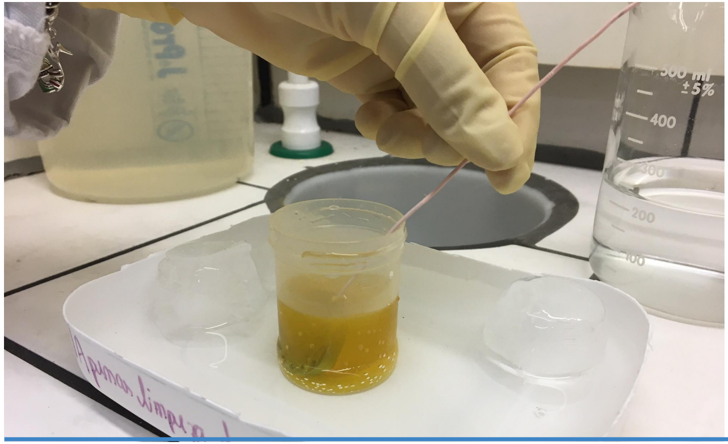

- The cavities were submitted to **chemical etching**, being dipped in a solution which composition in volume is as follow: HF (26%), HNO_3 (40%) and H_3PO_4 (34%).
- The aim is to **remove the first layers of the surface** that may have been contaminated during the fabrication process and layers of natural oxide.

Plasma immersion ion implantation (PIII) of Nitrogen.

- First step: sputtering with argon to prepare the sample;
- Second: PIII.

Collaboration with Dr. Rogério de Oliveira.

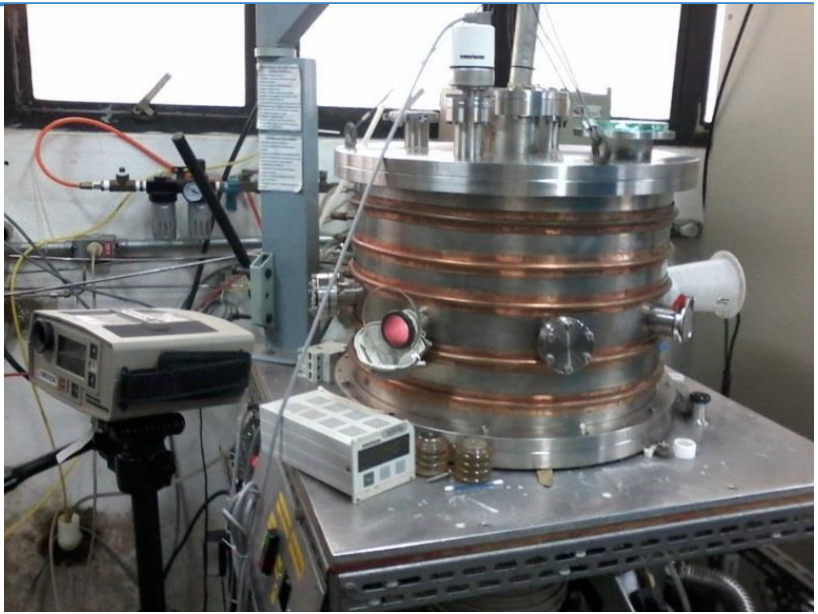

Measurements (semiquantitative): example of one **EDS** (Energy-dispersive X-ray spectroscopy).

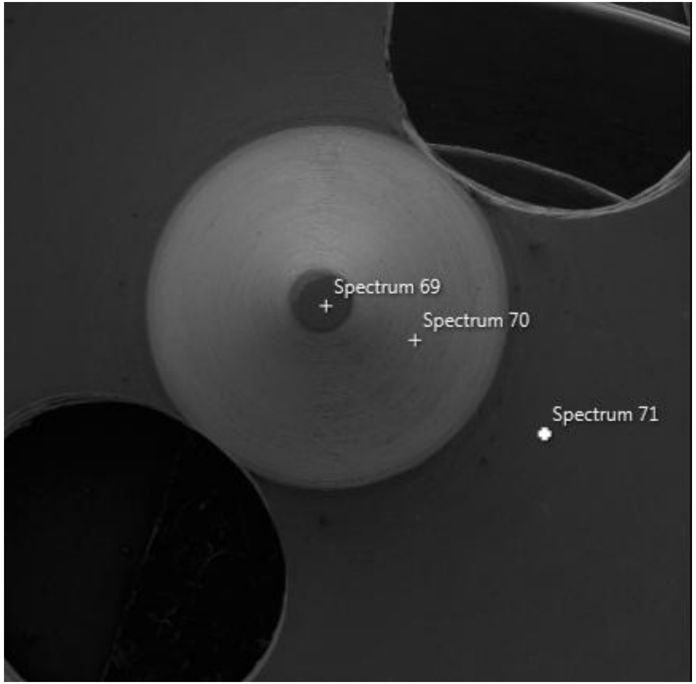

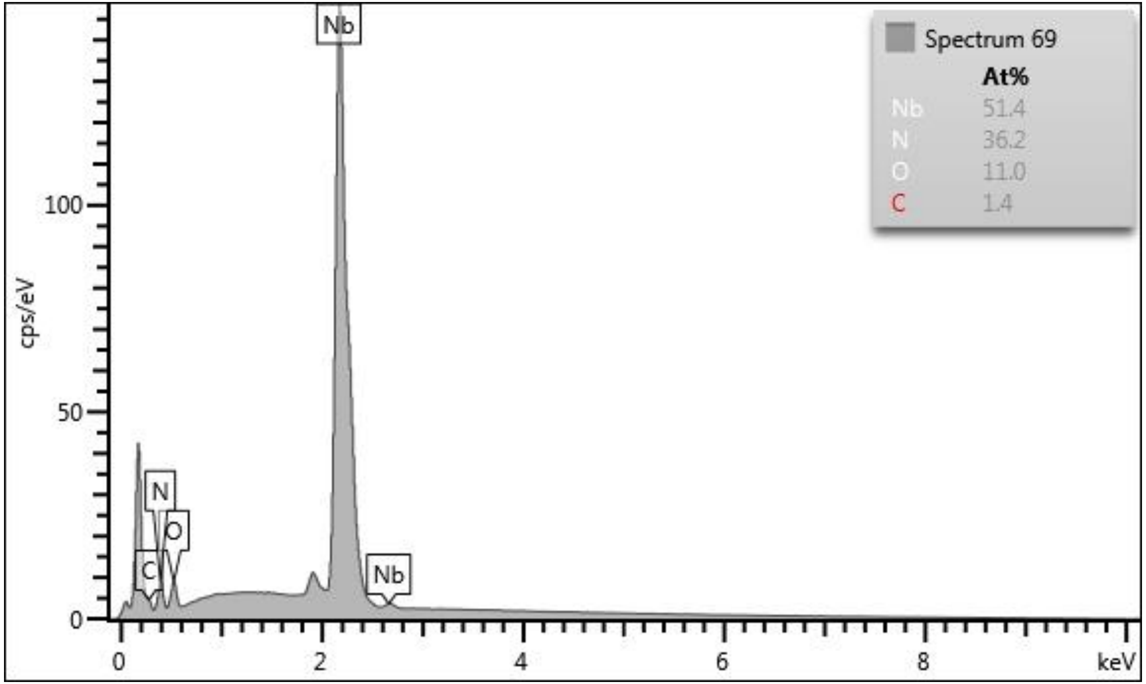

Sample 6.

- Measurements done by Dr. Michel Felipe.

Cryogenic measurements

Niobium transducers

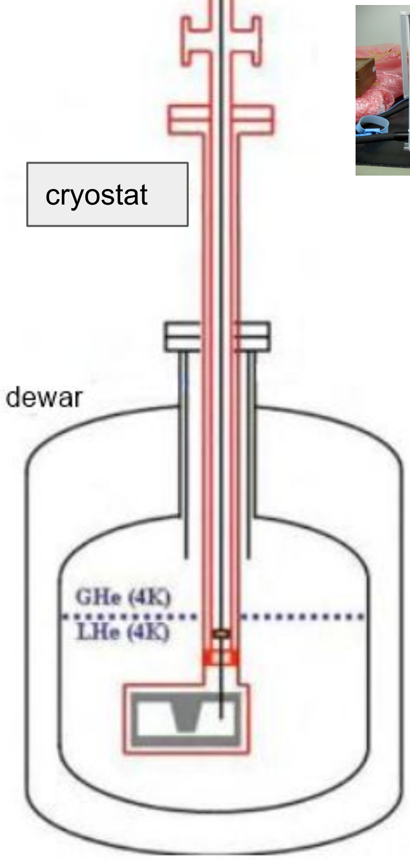

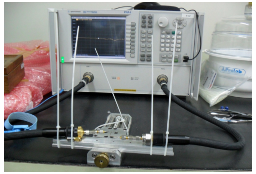

Cryogenic measurements

Niobium transducers

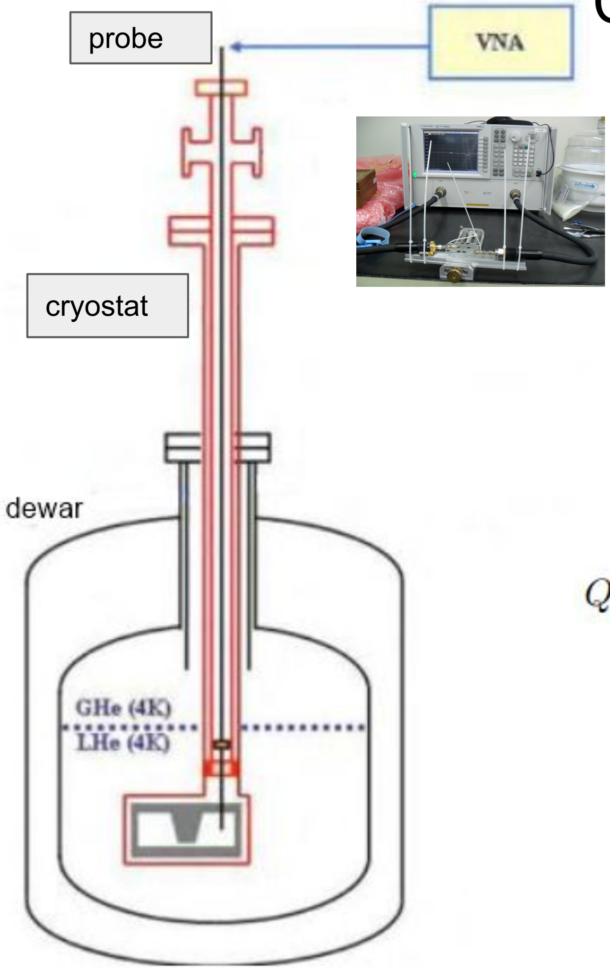

$$Q_{ec} = \frac{f_0}{\Delta f}$$

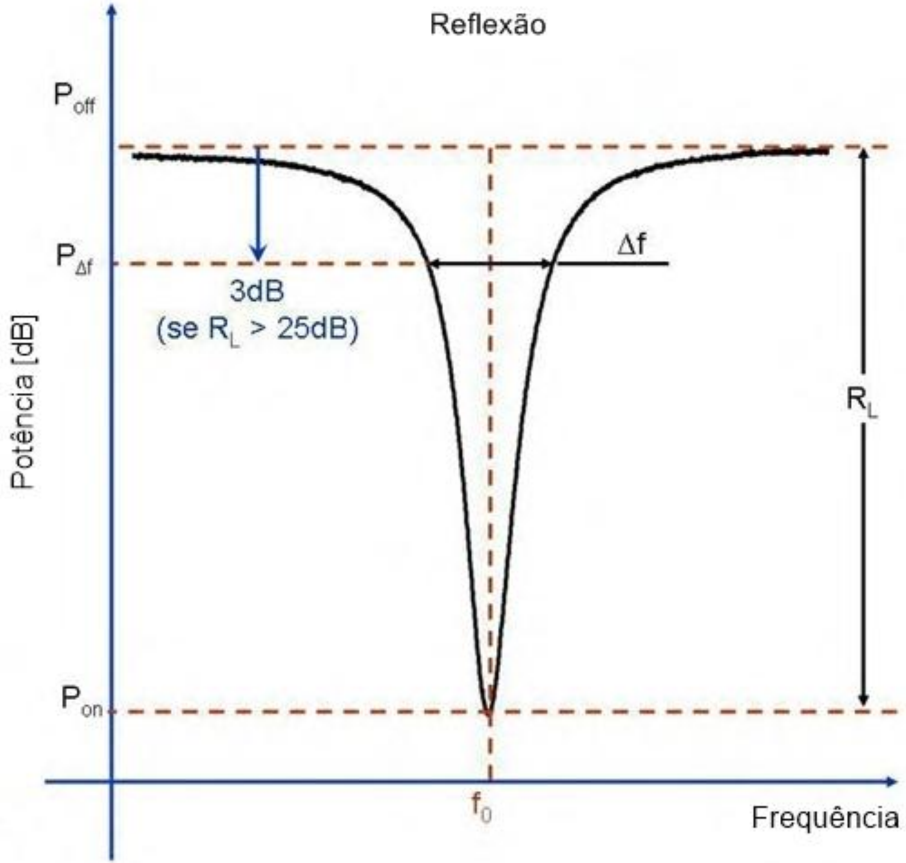

Example

Sample 10, Qe ≈ 50,000

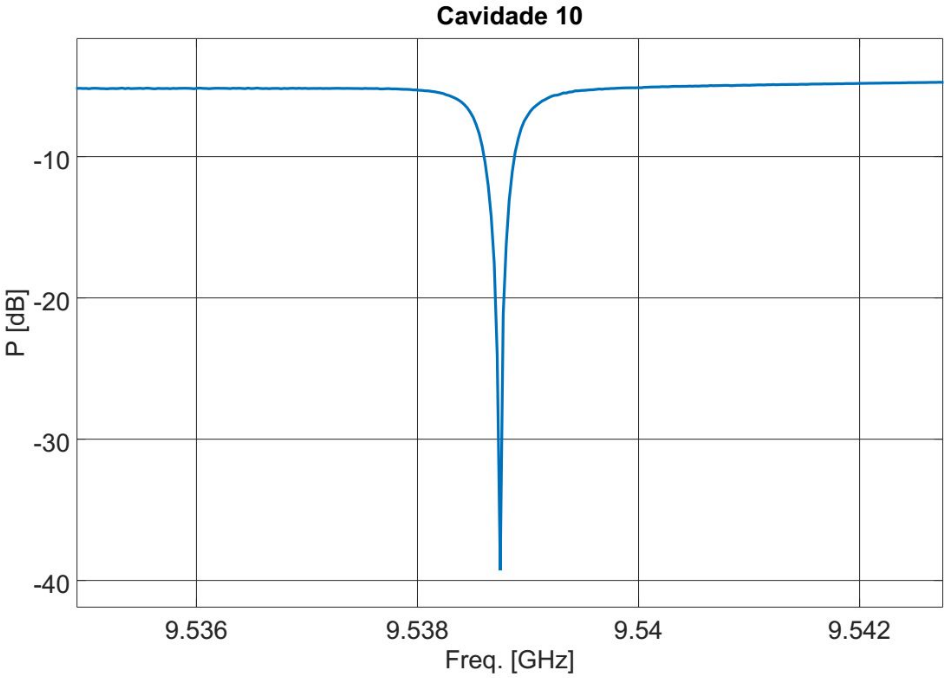

Tabela 3.3 - *Ranking* dos Q_e

Q_e	Amostra	N [%]		O [%]		C [%]		Tratamento inicial +
		P	T	P	T	P	T	
60185	2	2,1	4,2	9,1	2,7	25,0	5,6	1 AQC
54404	6	4,4	4,8	3,2	2,4	5,2	2,5	3 AQC
49935	10	3,1	4,6	2,9	2,4	7,6	5,6	3 AQC
26253	6	1,6	4,0	4,0	3,0	24	9,4	1 AQC
17795	3	24,8	18,6	4,4	3,8	0,5	10,1	1 AQC + 1 AQL + 3IP
13311	3	20,0	22,0	12,9	5,5	16,7	2,2	1 AQC + 1 AQL + 2x3IP
10704	8	4,9	4,2	18,0	32,0	2,3	2,4	1 AQC
9842	4	3,8	2,4	3,2	3,2	2,0	14,7	2 AQC
8711	8	5,0	4,1	28,2	37,5	3,9	5,0	-
7838	9	3,1	4,6	2,9	2,4	7,6	5,6	3 AQC
6181	5	2,8	4,6	4,0	4,2	9,4	5,4	2 AQC
5885	2	20,0	20,0	15,0	8,7	33,0	23,0	-
5215	3	0,4	4,2	18,0	2,8	58,0	3,6	1 AQC
4846	1	0,7	3,3	18,8	3,4	24,0	6,9	1 AQL + 2x3IP
4449	10	41	35	9,6	8,5	6,2	9,4	-
3982	6	36	28	11	16	1,4	13	-
3978	4	41,6	32,2	3,4	14,4	2,1	4,2	-
2061	3	24	30	11	8,5	19	5,1	-
1936	2	3,4	2,4	4,0	2,4	3,7	8,1	2 AQC
1537	1	8,0	28,7	30,4	4,0	30,0	2,2	1 AQL + 3IP
1230	9	44	25	7,3	6,1	0,0	9,5	-

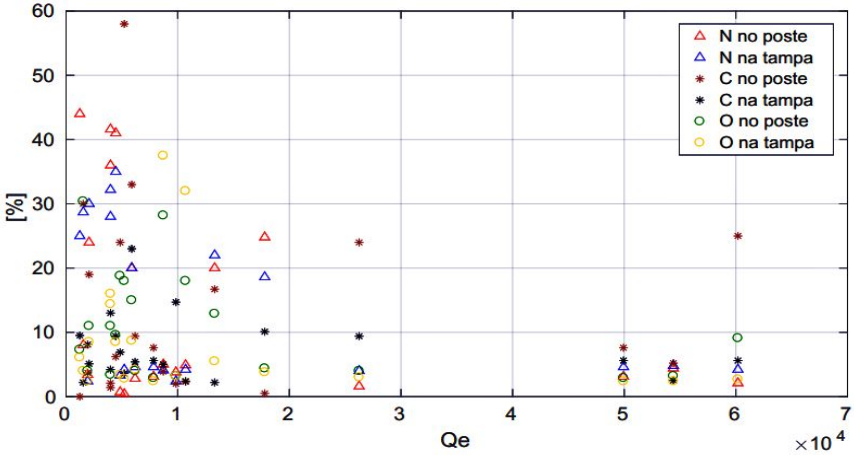

Partial conclusions

- The electrical resonance frequencies of the transducers were adjusted to good values to be **in operation** on Schenberg detector.
- The highest Qe for the surface treatment was around **60,000**.
- It was observed that **low atomic percentages**, of nitrogen and carbon and oxygen, on the surfaces of niobium cavities are probably a requirement for obtaining **higher Qe’s**.

- A **master student is now working with anodization** in order to create a protection layer at the surface and obtain higher Qe’s. **It has been reported Qe ~ 170,000**.

Multi-Nested Pendula for interferometric detectors

Advanced LIGO

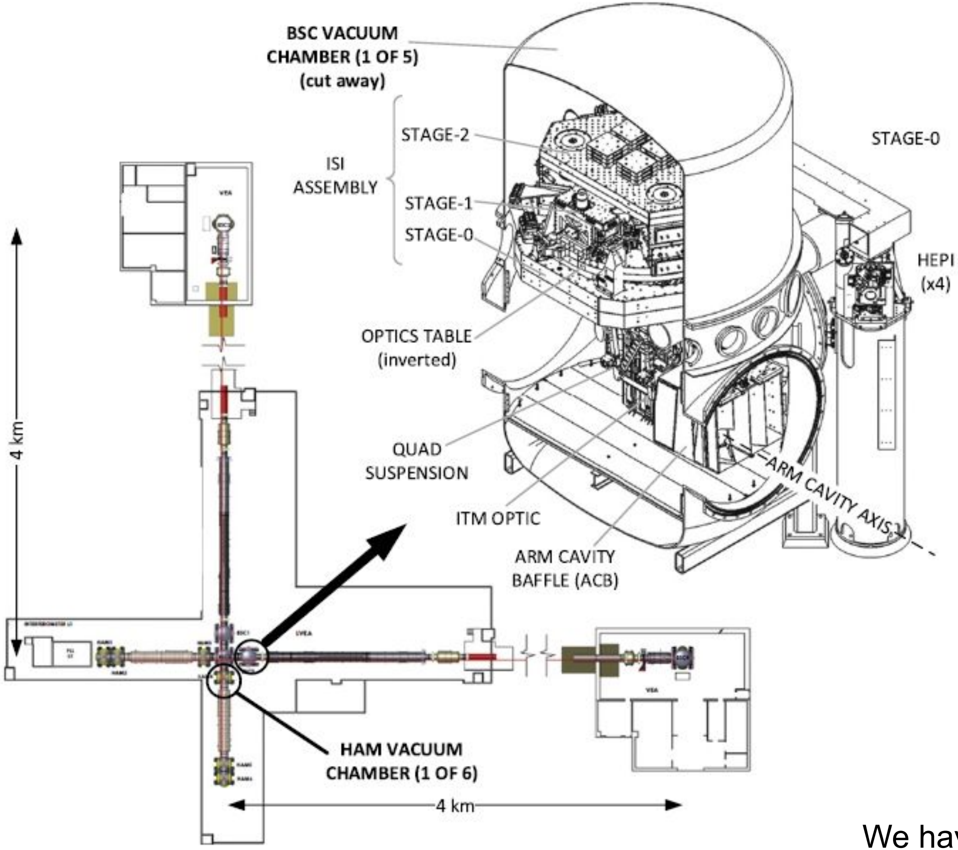

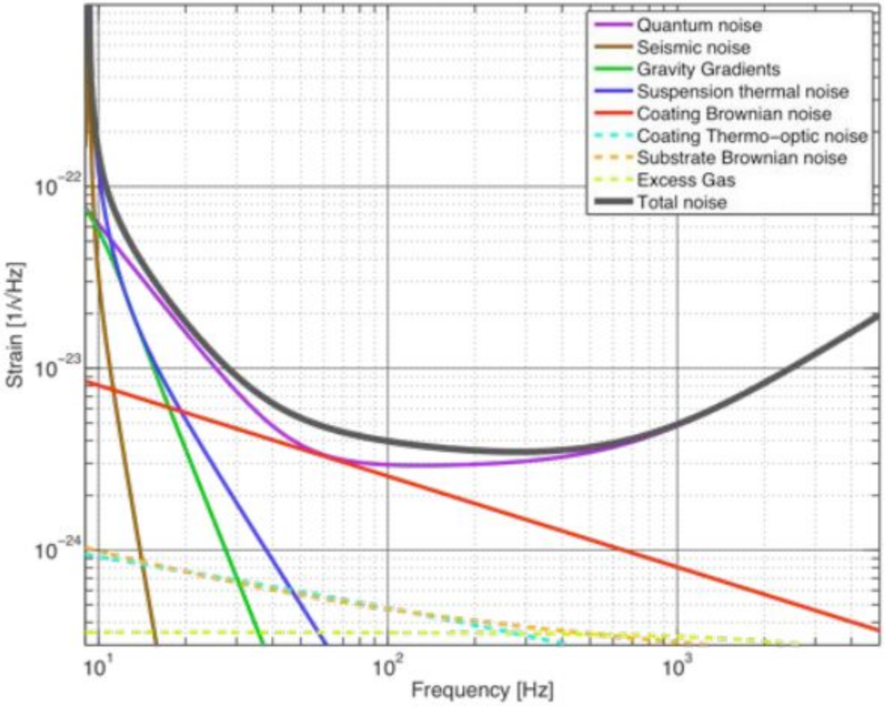

We have persistent ground vibrations and a seismic wall below 10 Hz.

Multi-Nested Pendula

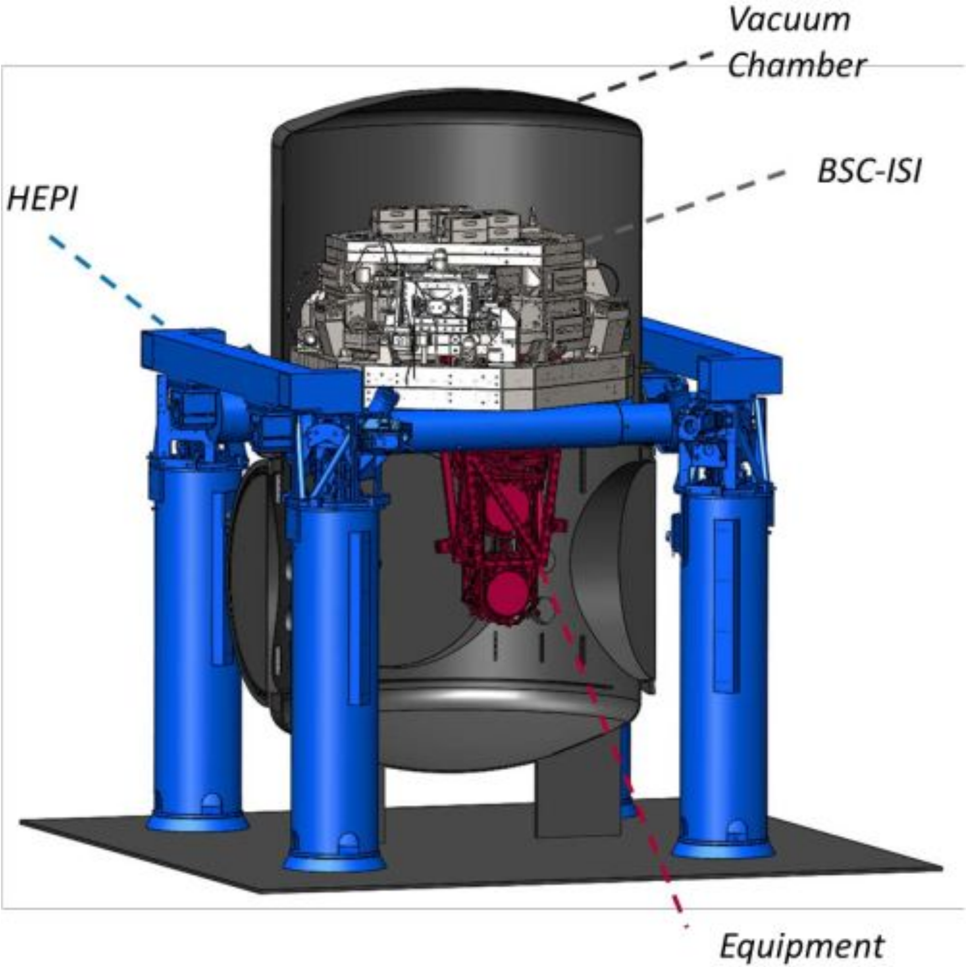

Multi-Nested Pendula

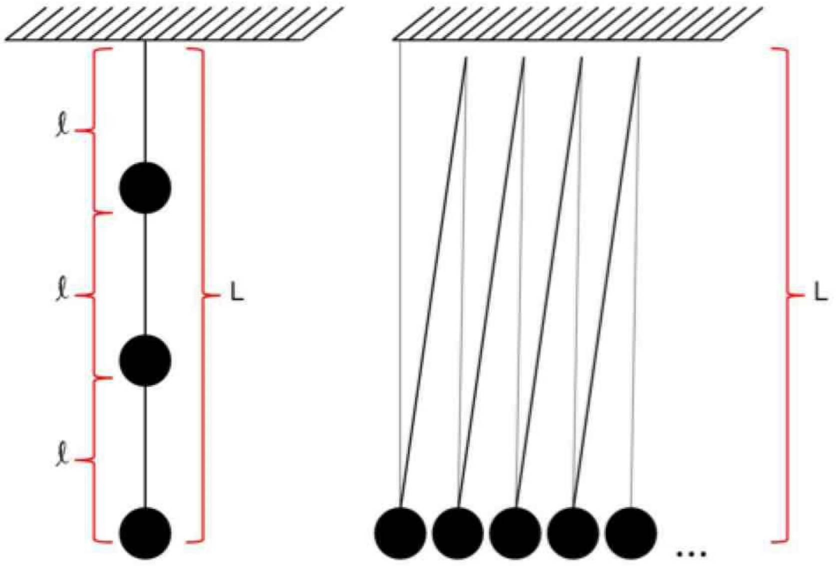

$$\frac{x}{x_e} \approx \left(\frac{f_0^2}{f^2}\right)^N , \text{ for } \quad f \gg f_0$$

Multi-Nested Pendula (MNP)

It’s proposal instrument to work like a N-stages cascaded system, however, saving vertical space.

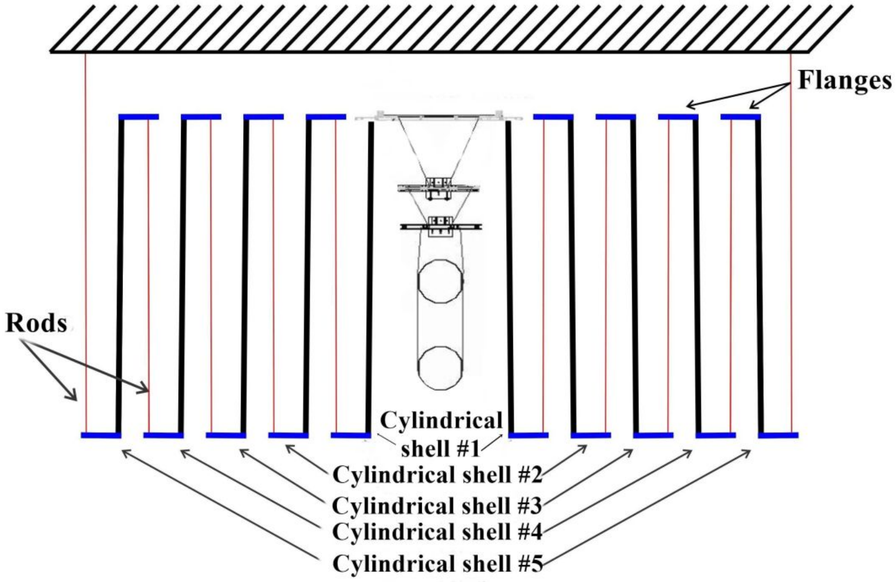

Dr. Márcio Constâncio Jr near the initial MNP prototype, INPE, Brazil.

https://arxiv.org/abs/1304.1393
http://dx.doi.org/10.1088/1748-0221/9/08/T08006

Vertical vibration isolation for MNP

After some theoretical studies and also tests using pneumatic springs, we decided to investigate Geometric Anti-Springs (GAS).

Left: design of the initial GAS prototype for the MNP. Right: views of the GAS prototype with an additional stage to adjust the working point to the equilibrium point, for the given load.
The blades of the additional stage are not bent like those in GAS stage (like a fishing rod). They just add a vertical spring constant.
An aluminum piece connects the GAS unit to its additional stage.
They are 22 cm diameter and the blades are made of stainless steel (AISI 301, HRC 40-45).

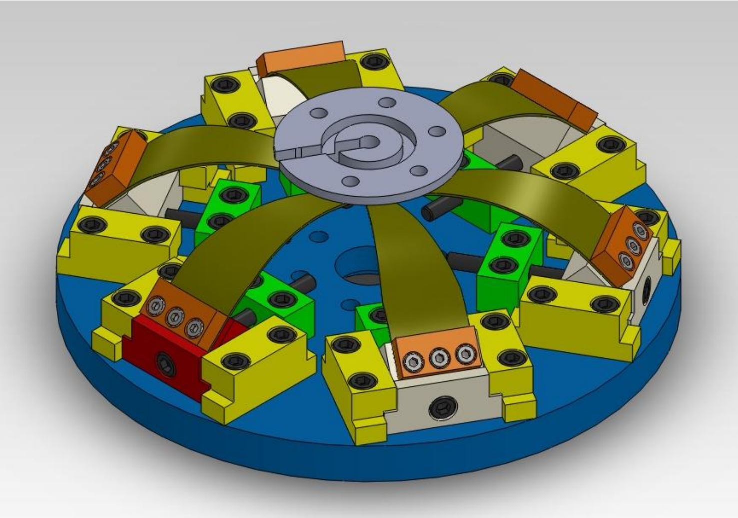

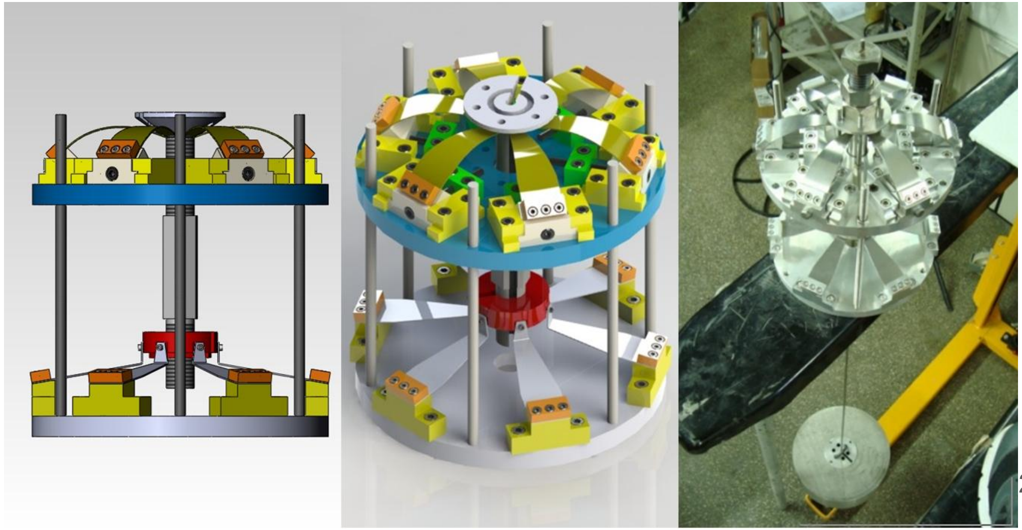

GAS

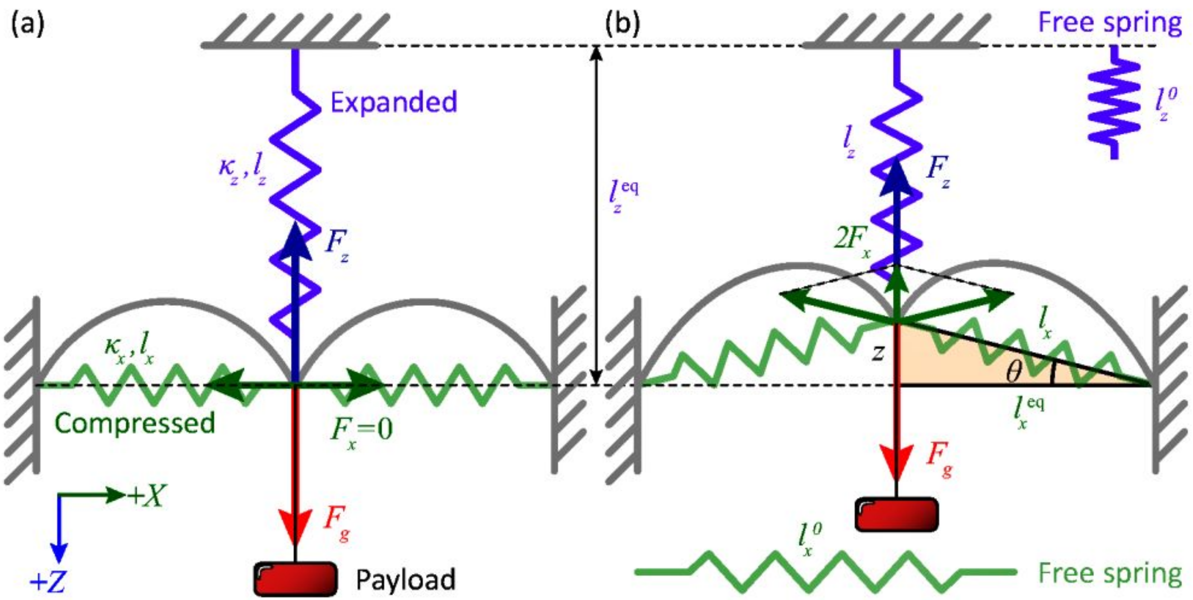

$$k_{\text{eff}} = k_z + k_x \left(\frac{l_x - l_x^0}{l_x} \right)$$

For two stages (our case):

$$k'_{\text{eff}} = k_z + k_{z(\text{add})} + k_x \left(\frac{l_x - l_x^0}{l_x} \right)$$

Tests and measurements

- We have tested different configurations of how GAS blades connect to the center disc.
- We use a **PZT sensor glued to a blade** to measure the resonance frequencies.
- The **quietest platform** used is show in the figure.
- The PZT signal were read by a **SR760 FFT spectrum analyzer**.
- About 60 kg payload was suspended by a rod, 1.3 m long and 6.4 mm thick.

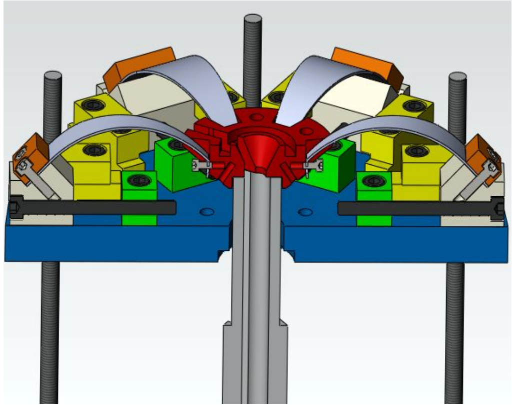

Cross-sectional view of the GAS with the central disc in red. In this final configuration, we screwed the blade tip to the inner wall of a cut made in the central disc.

Results

Compression (mm)	f_0 (Hz)	Mechanical Q factor
0	7.58	166 ± 12
1	7.34	117 ± 7.1
2	6.97	140 ± 11
3	7.09	157 ± 14
4	6.85	119 ± 6.7
5	6.72	127 ± 10
6	6.36	117 ± 8.8
7	6.12	111 ± 4.5
8	5.87	113 ± 3.0
9	5.50	108 ± 5.6
10	4.77	104 ± 6.3
11	4.65	104 ± 2.8
12	4.53	96.0 ± 1.3
13	4.15	84.8 ± 3.0
14	3.91	74.6 ± 2.3
15	3.91	–
16	4.15	80.3 ± 1.8
17	4.77	90.6 ± 3.8
19	5.38	90.7 ± 5.5
20	6.73	105 ± 6.4
21	6.97	105 ± 5.7
22	7.21	101 ± 6.8
23	7.70	98.7 ± 5.9
24	7.95	102 ± 4.7

GAS effect: f_0 from 7,58 to 3,91 Hz.

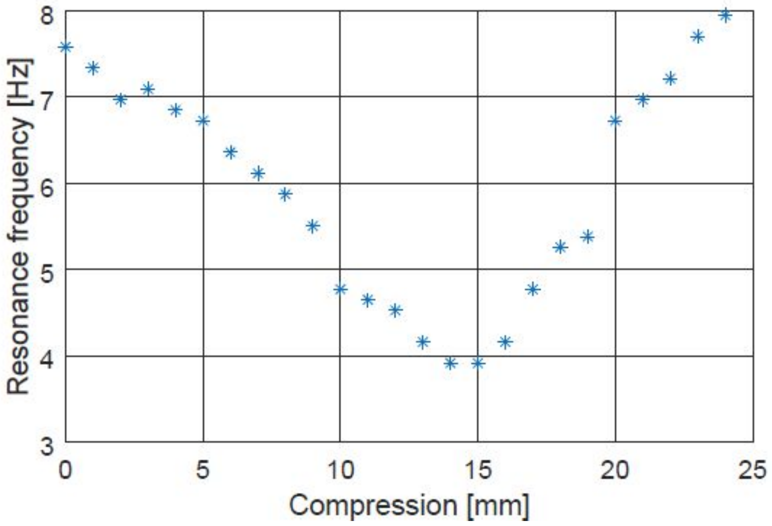

Estimated by $Q \approx 2,72 f_0 \tau_{10\mathrm{dB}}$

MNP with GAS

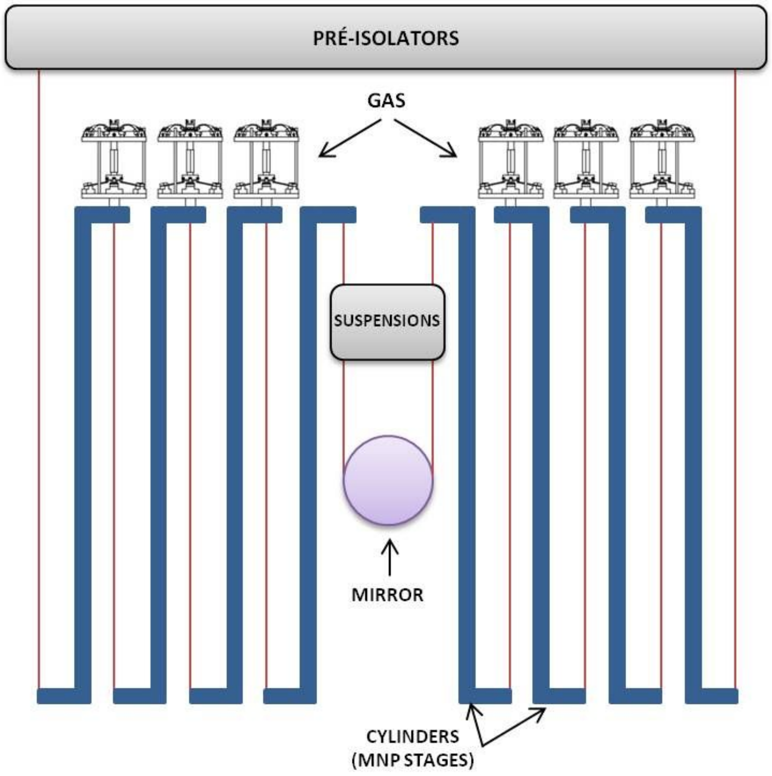
PRÉ-ISOLATORS
GAS
SUSPENSIONS
MIRROR
CYLINDERS
(MNP STAGES)

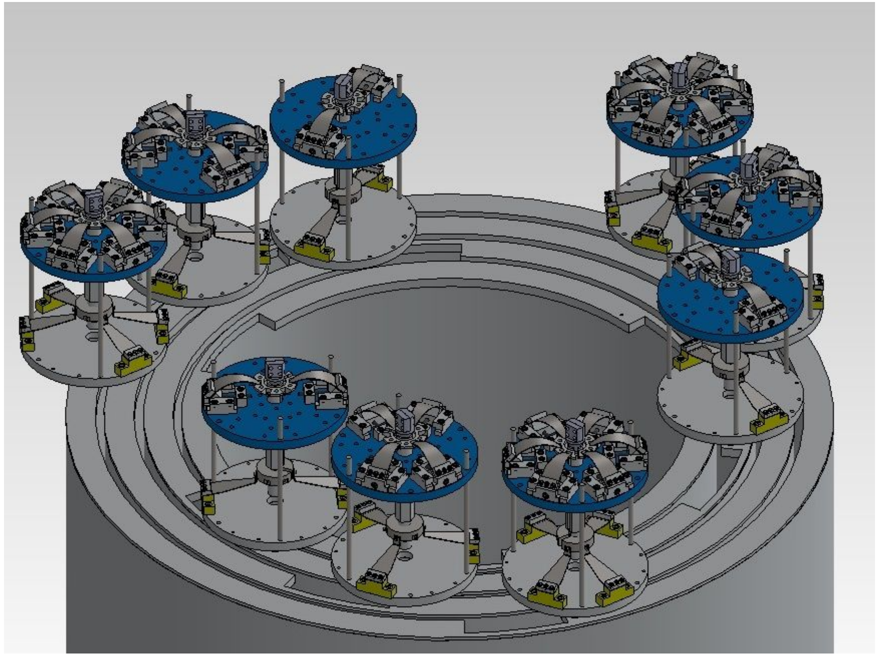

How to install GAS in the MNP?

More improvements:

- Center of Percussion (CoP) considerations: new shell model.
- New suspensions.

Ti-6Al-4V wires and *music wires* (no more rods).

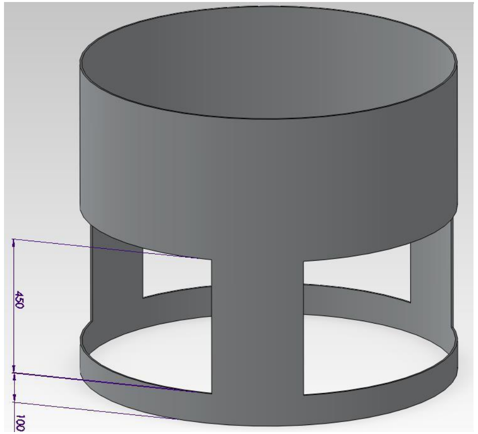

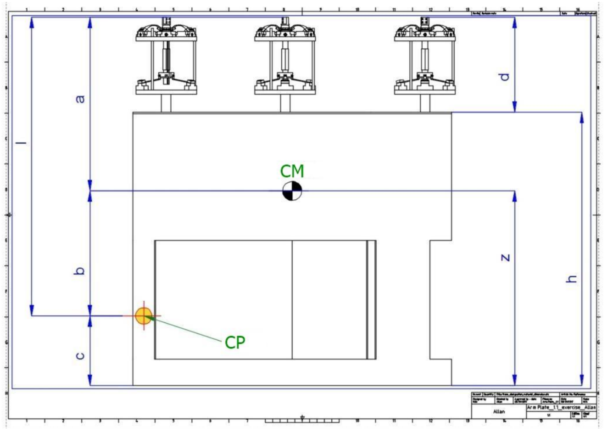

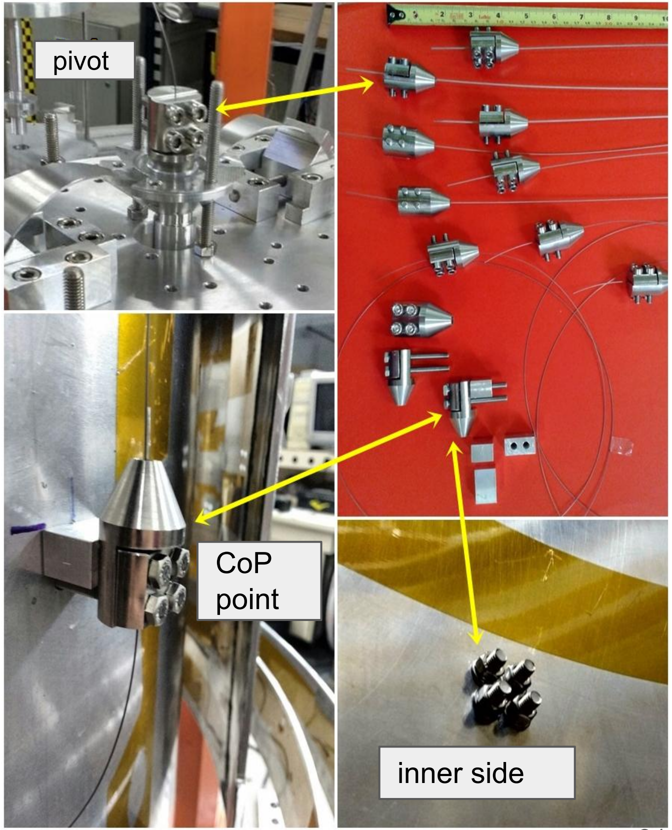

Preparing the system to be measured

- Sensors: two TC120 placed on the center of mass of the inner shell and of the outer shell.
- Soft cable connections to the sensors.
- System inside the vacuum chamber.

More relevant results

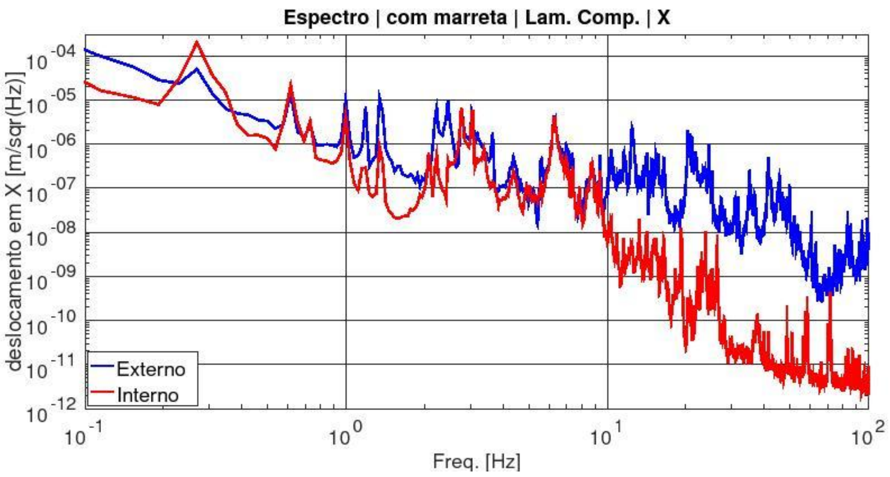

- MNP reveals pendulum resonance peaks at low frequencies (<2 Hz), and vertical springs resonance peaks between 2 and 10 Hz.
- At frequencies > 40 Hz, the the inner stage reach the sensitivity limit of the sensors.
- The system reveals better attenuation from 10 Hz on the horizontal axis, and from 20 Hz on the Z axis. The attenuation reaches a factor of the order of 10^4 in some regions.
- Simulations also revealed an attenuation of around 10^4.

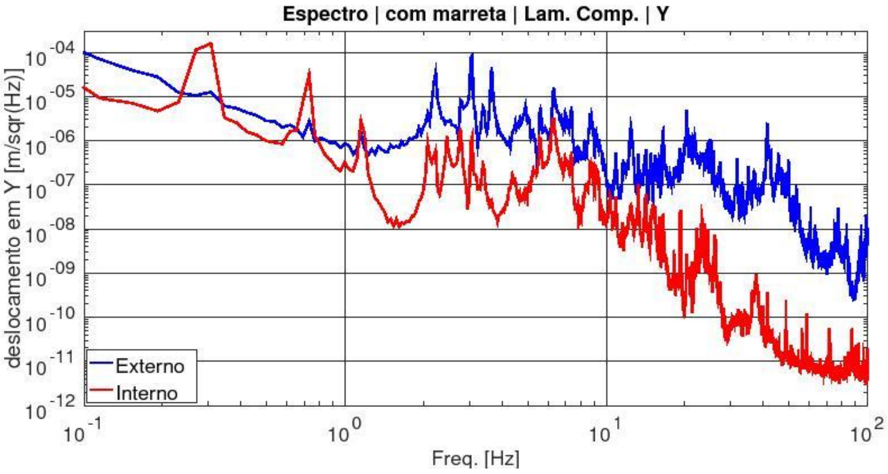

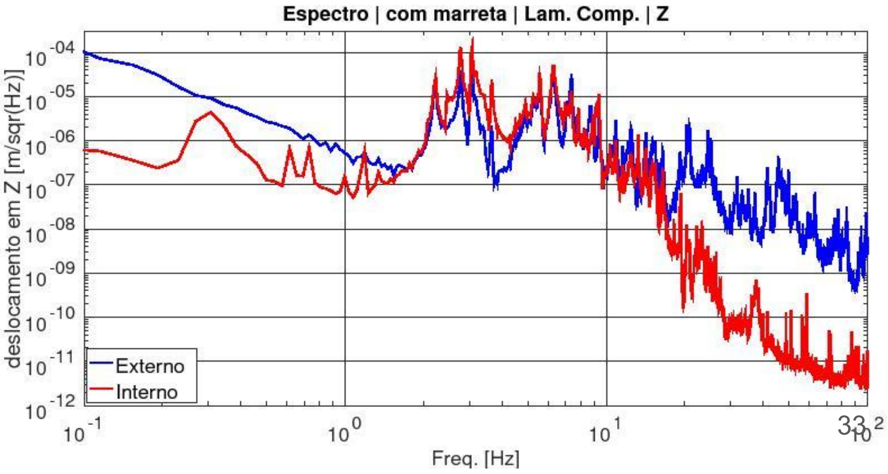

Partial conclusions

- We have **verified the GAS effect** in our two-stage prototype. It was possible to test a wide range of compression levels of the blades, and we had a reduction in the fundamental resonance frequency of almost 50%.
- MNP seismic measurements reveal greater attenuation **from 10 Hz** on the horizontal axis, and **from 20 Hz** on the vertical axis.
- The **attenuation reaches a factor of the order of 10^4** in some regions. It could be better, if there were no resonant peaks in the vibrational modes of the cylindrical shells.
- This was the **first time that the TF’s** of the optimized cylindrical MNP **were obtained**.

Thank you for your attention!

elvis.camilo@uclouvain.be

Extra slides

Teste C: lâminas parafusadas lateralmente

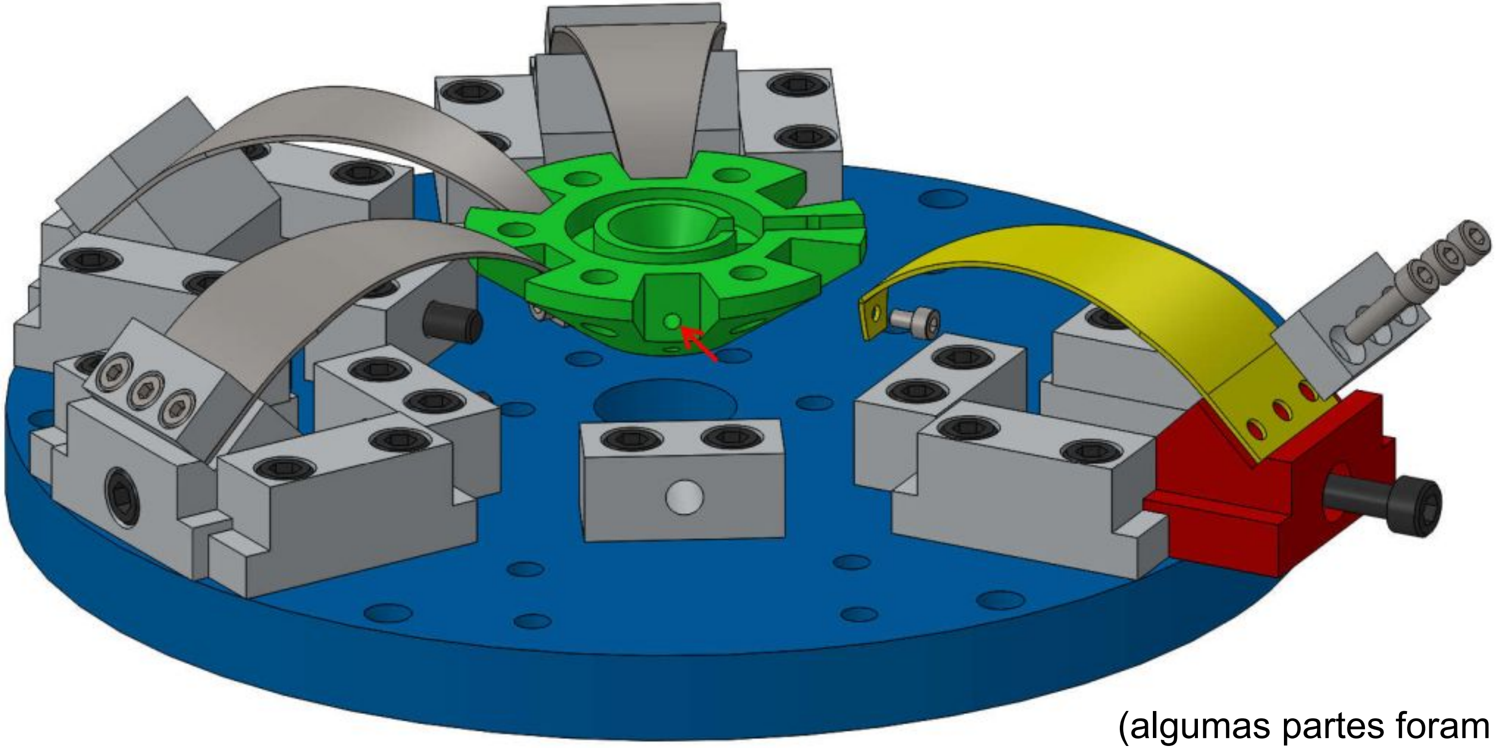

(algumas partes foram omitidas)

Center of percussion

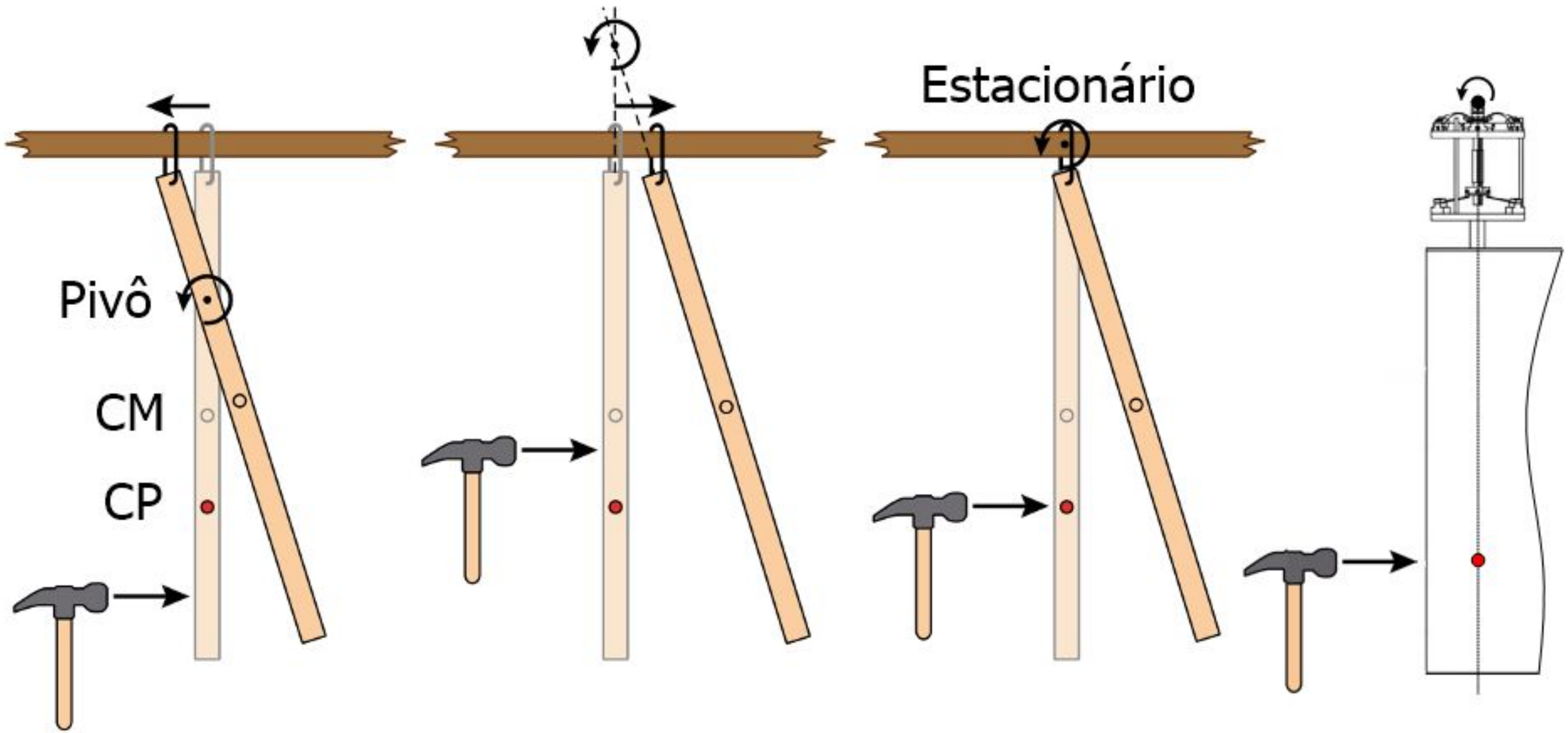

Center of percussion

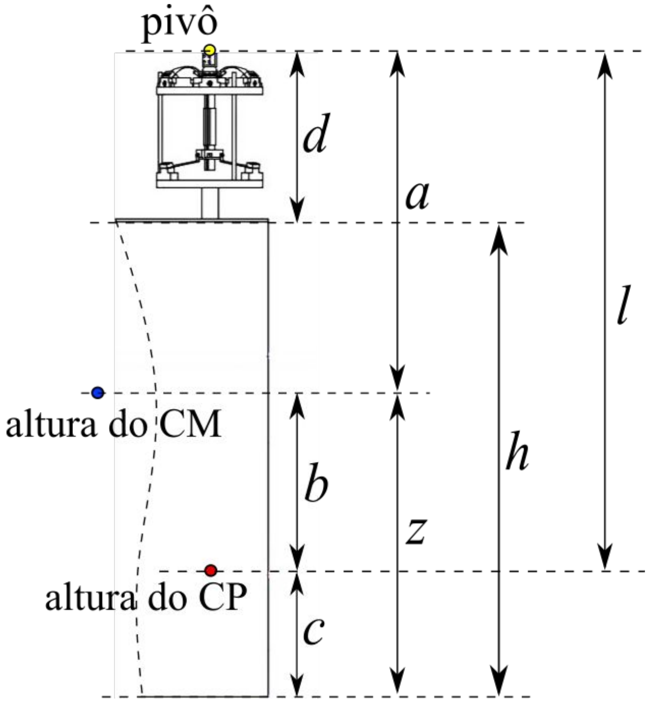

$$b = \frac{1}{a}\frac{L}{m}$$

L is the moment of inertia.

Medições vibracionais com aplicação de uma força externa

bobina, alto-falante, marreta
3 experimentos: sem compressão; com compressão; e sem lâminas no estágio adicional

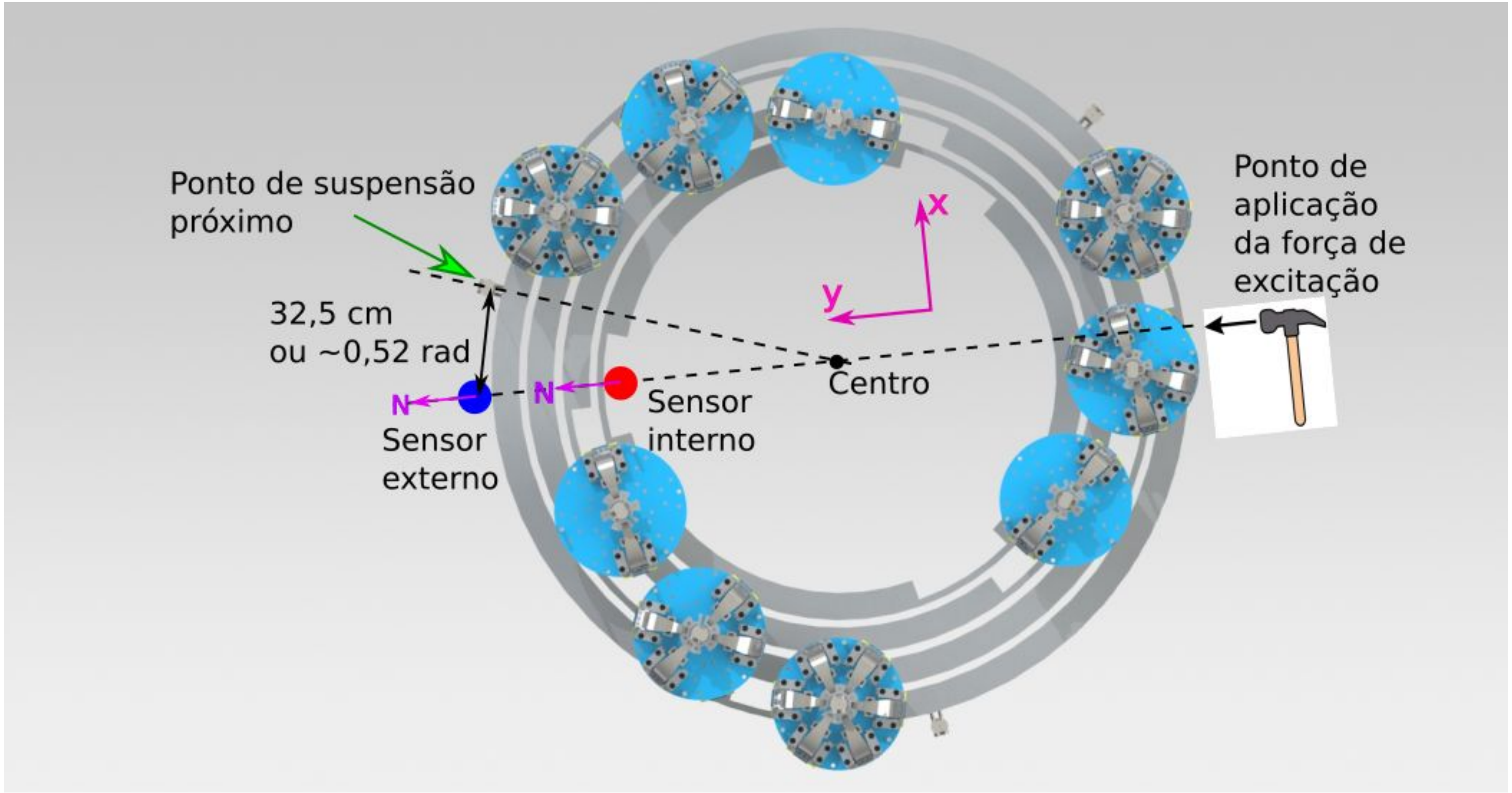

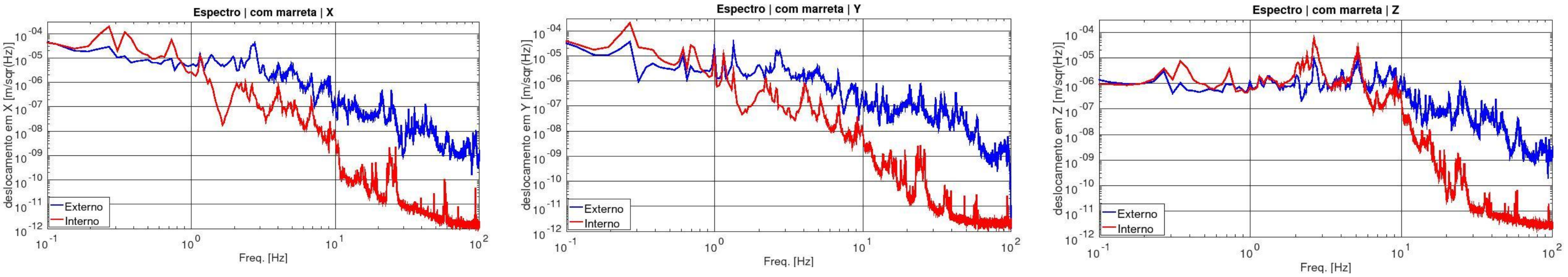
Espectro | com marreta | X
deslocamento em X [m/sqr(Hz)]
Freq. [Hz]
Externo
Interno
Espectro | com marreta | Y
deslocamento em Y [m/sqr(Hz)]
Freq. [Hz]
Externo
Interno
Espectro | com marreta | Z
deslocamento em Z [m/sqr(Hz)]
Freq. [Hz]
Externo
Interno

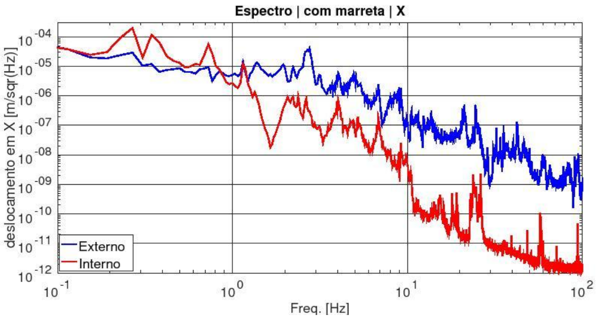
Espectro | com marreta | X
deslocamento em X [m/sqr(Hz)]
Freq. [Hz]
Externo
Interno

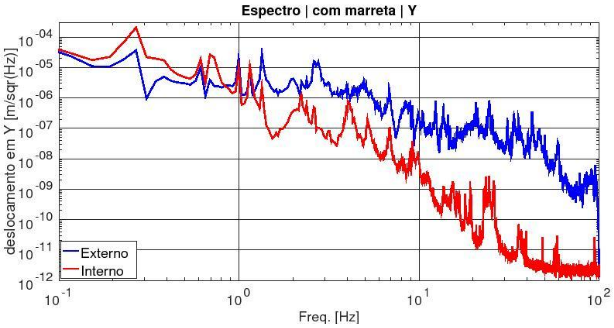
Espectro | com marreta | Y
deslocamento em Y [m/sqr(Hz)]
Freq. [Hz]
Externo
Interno

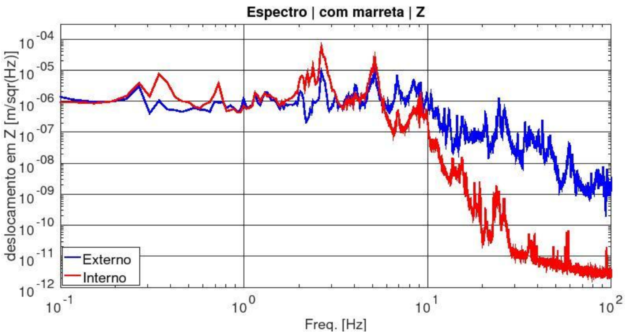
Espectro | com marreta | Z
deslocamento em Z [m/sqr(Hz)]
Freq. [Hz]
Externo
Interno

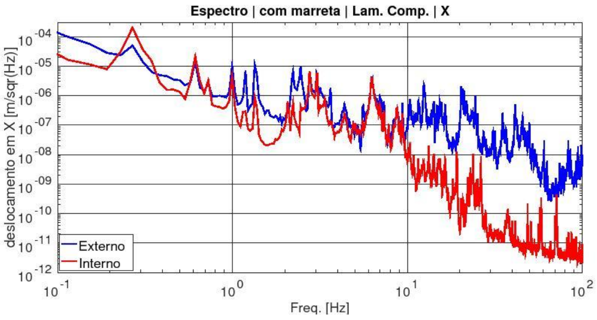
Espectro | com marreta | Lam. Comp. | X
deslocamento em X [m/sqr(Hz)]
Freq. [Hz]
Externo
Interno

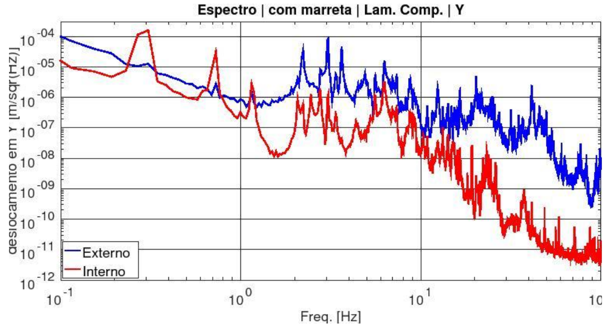
Espectro | com marreta | Lam. Comp. | Y
deslocamento em Y [m/sqr(Hz)]
Freq. [Hz]
Externo
Interno

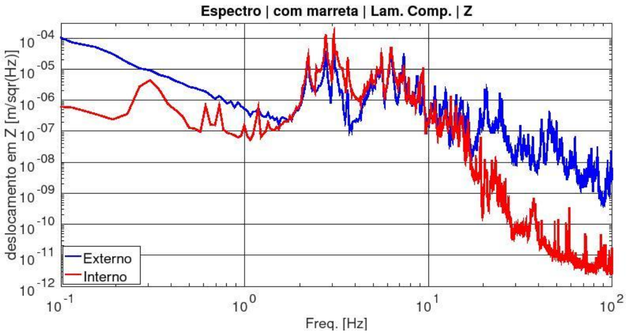
Espectro | com marreta | Lam. Comp. | Z
deslocamento em Z [m/sqr(Hz)]
Freq. [Hz]
Externo
Interno

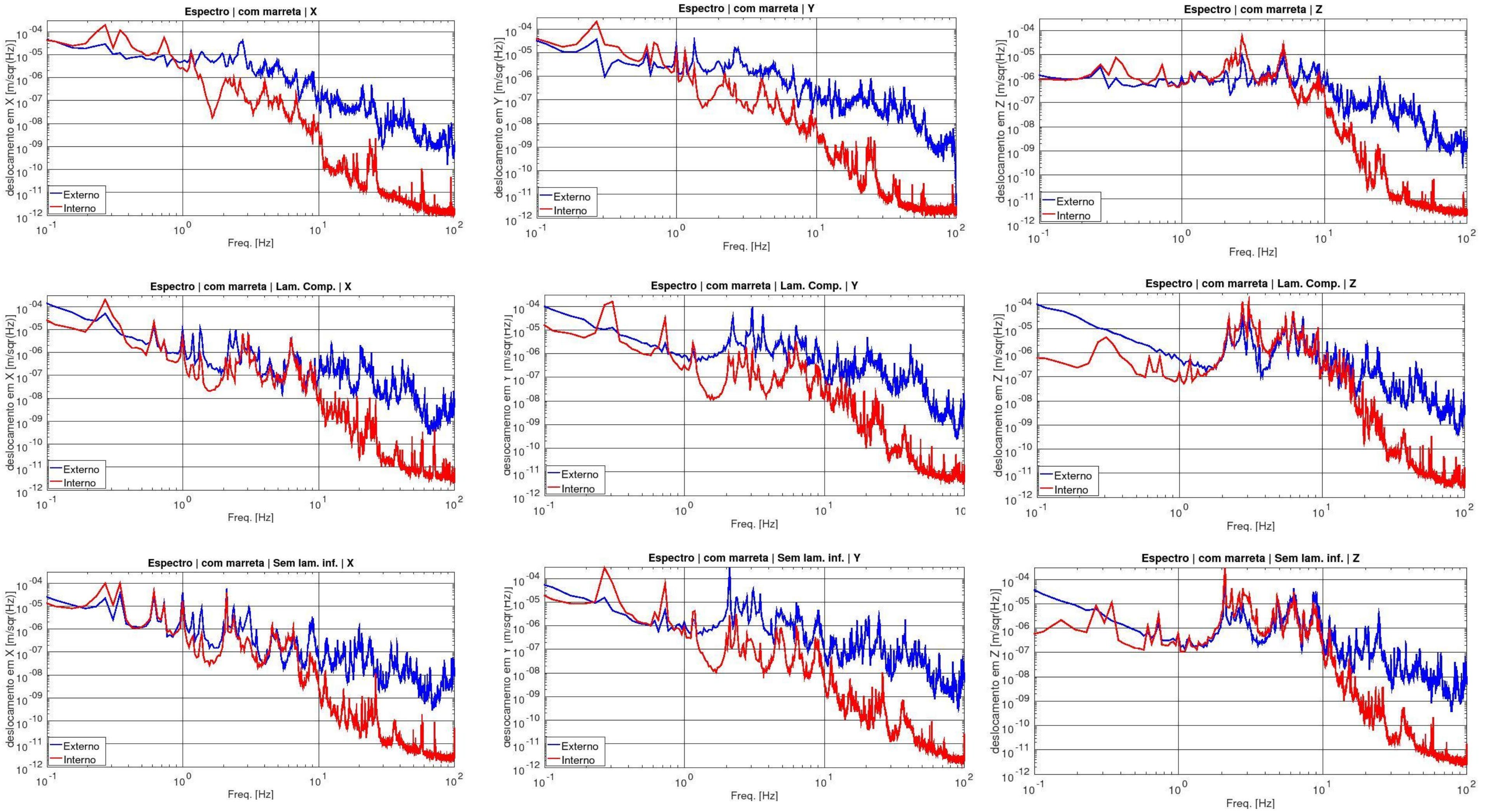

Espectro | com marreta | X
Espectro | com marreta | Y
Espectro | com marreta | Z
Espectro | com marreta | Lam. Comp. | X
Espectro | com marreta | Lam. Comp. | Y
Espectro | com marreta | Lam. Comp. | Z
Espectro | com marreta | Sem lam. inf. | X
Espectro | com marreta | Sem lam. inf. | Y
Espectro | com marreta | Sem lam. inf. | Z
deslocamento em X [m/sqr(Hz)]
deslocamento em Y [m/sqr(Hz)]
deslocamento em Z [m/sqr(Hz)]
Freq. [Hz]
Externo
Interno

Comparando os resultados com simulações

Tabela 4.7 - Valores utilizados nas simulações do MNP otimizado com GAS

	Estágio	Massa acumulada, M [kg]	Conjunto de molas	f_0 da mola [Hz]	k da mola [N/mm]
Simulação 1	1	241,2	-	-	-
	2	170,4	1º	7,50	126,1
	3	106,3	2º	7,50	78,7
	4	51,6	3º	7,50	38,2
Simulação 2	1	241,2	-	-	-
	2	170,4	1º	3,90	34,1
	3	106,3	2º	3,90	21,3
	4	51,6	3º	3,90	10,3

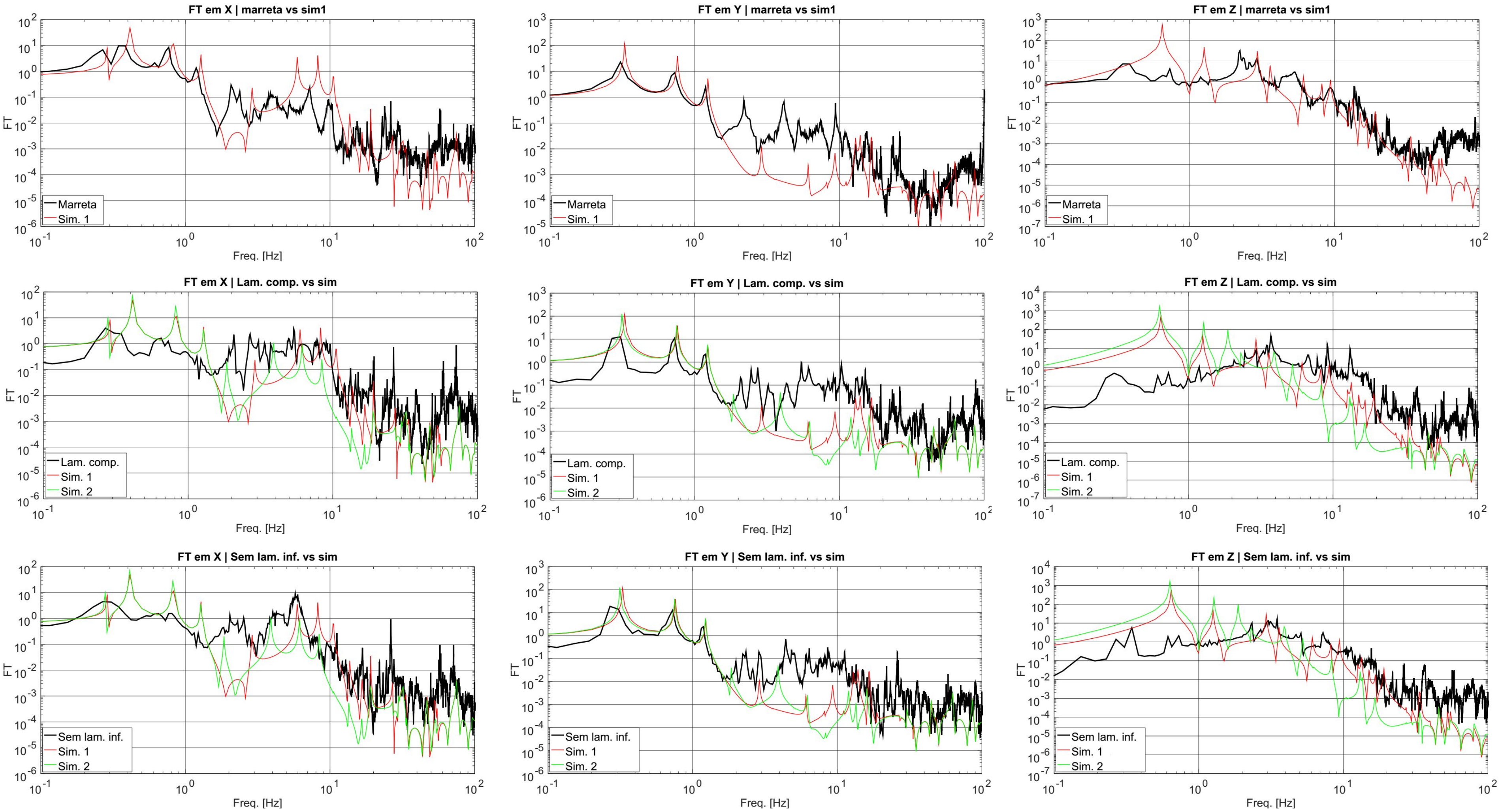
FT em X | marreta vs sim1
FT em Y | marreta vs sim1
FT em Z | marreta vs sim1
Marreta
Sim. 1
FT em X | Lam. comp. vs sim
FT em Y | Lam. comp. vs sim
FT em Z | Lam. comp. vs sim
Lam. comp.
Sim. 1
Sim. 2
FT em X | Sem lam. inf. vs sim
FT em Y | Sem lam. inf. vs sim
FT em Z | Sem lam. inf. vs sim
Sem lam. inf.
Sim. 1
Sim. 2
FT
Freq. [Hz]